PHYSICAL REVIEW B VOLUME 57, NUMBER 8 15 FEBRUARY 1998-II

Antimony adsorption on InAs(110)

Maria Grazia Betti, Vincenzo Martinelli, and Carlo Mariani
Istituto Nazionale per la Fisica della Materia, Dipartimento di Fisica, Università di Modena, Via G. Campi 213/A, I-41100 Modena, Italy
(Received 8 September 1997)

The overlayer growth of the Sb/InAs(110) interface has been investigated for room-temperature (RT) deposition and subsequent annealing, by means of Auger and core-level photoemission spectroscopy. Antimony forms an unreactive and epitaxial monolayer, followed by three-dimensional island growth. The surface electronic transitions above the semiconductor bulk gap and Sb-induced electronic states have been studied by means of photoemission and high-resolution electron-energy-loss spectroscopy. The Sb/InAs(110) interface is semiconducting and the (1×1) Sb structure, obtained after a thermal annealing at 600 K, presents a surface band gap of 0.42 eV at RT. Schottky barrier height, derived from the energy shift of the In core-level emission lines, is about 0.7 eV with respect to the valence-band maximum. The evolution of the space-charge layer with the formation of an accumulation layer has been deduced from the dopant-induced free-carrier plasmon. The accumulation layer and the Schottky barrier height are reduced when the annealing procedure reorders the surface to obtain the (1×1) two-dimensional structure. [S0163-1829(98)01707-X]

I. INTRODUCTION

The adsorption of column V elements on the (110) surface of III–V compounds has been the topic of extensive experimental and theoretical work.[1,2] The scientific interest is due to the formation of unreactive and ordered two-dimensional (2D) structures that are appealing candidates on which to compare theoretical predictions[1,3,4] and experimental results.[2,5–8] A large amount of experimental and theoretical work has been devoted to study the model system Sb/GaAs(110) that presents an epitaxial continued layer structure[6,9] (ECLS) preserving the semiconductor character of the interface.[6,8,10] Only a few results are available on the adsorption of semimetals on narrow-gap III–V (110) with a large lattice constant like InAs(110), InSb(110), and GaSb(110).[11–13] A preliminary study by Ford *et al.*[11] states that antimony deposited on InSb(110) and GaSb(110) does not lead to an epitaxial and ordered interface, while InAs(110) seems a good candidate to verify the consistency of the ECLS model for these 2D systems. Although the InAs(110) surface presents a large surface unit cell ($a_0 = 6.06$ Å), the Sb chains form as well an epitaxial continued layer structure, as deduced by photoelectron diffraction[12] and confirmed by total-energy calculation,[13] with the Sb-Sb distance of 2.72 Å matching with the In-As bond length of the underlying chains. Considering the ECLS atomic geometry for the (1×1)-Sb/InAs(110) interface, the band structure has been calculated,[4,13] finding Sb-induced filled states (S5 and S6) close to the valence-band maximum (VBM), and empty levels (S7 and S8) close to the conduction-band minimum (CBM), conserving the topological band picture of the surface states in the clean InAs(110) surface.

In the present work we study the growth morphology of Sb on InAs(110) and of the (1×1)-Sb ordered layer by means of Auger electron spectroscopy and analyze the surface bonding by core-level photoemission spectroscopy. The room-temperature growth morphology of Sb on InAs(110) is characterized by unreactivity and lack of interdiffusion and preferential bonding sites. After completion of a first laminar monolayer, antimony forms disordered islands. Annealing at 600 K produces a highly ordered (1×1)-Sb monolayer structure. The surface electronic transitions above the semiconductor bulk gap and Sb-induced electronic states have been studied by means of photoemission and high-resolution electron-energy-loss spectroscopy (HREELS). The (1×1)-Sb/InAs(110) has a surface band gap of 0.42 eV at RT. The Schottky barrier height and the evolution of the space-charge layer have been deduced from core-level photoemission and dopant-induced free-carrier plasmon, leading to the formation of an accumulation layer. After the annealing of a thick Sb layer, the accumulation layer is reduced and the (1×1)-Sb 2D ordered structure shows nearly flat bands.

II. EXPERIMENT

The experiments, carried out at the surface physics laboratory S.E.S.A.MO. at the Dipartimento di Fisica, Università di Modena, were performed in an Ultrahigh vacuum chamber containing a high-resolution monochromator-analyzer spectrometer (Leybold Heraeus ELS 22), ultraviolet photoelectron spectroscopy, and other ancillary facilities for sample preparation. Base pressure was kept below 10^{-10} mbar (10^{-8} Pa).

Photoelectron spectra were recorded using a He discharge lamp (He I photons, $h\nu = 21.2$ eV, He II, $h\nu = 40.8$ eV) with a grazing incidence angle. The photoemitted electrons were analyzed with an angle integrating cylindrical mirror analyzer used at constant energy resolution. The Fermi level was determined on a Sb thick layer. The overall experimental resolution, deconvoluted from thermal broadening, was better than 80 meV. The Auger electrons were collected in the first derivative mode, with a 1-V voltage modulation and the primary beam energy at 2 keV. HREELS measurements were performed in specular geometry with primary beam energies ranging between 5 and 22 eV and with an overall resolution of about 12 meV.

0163-1829/98/57(8)/4544(8)/$15.00 © 1998 The American Physical Society

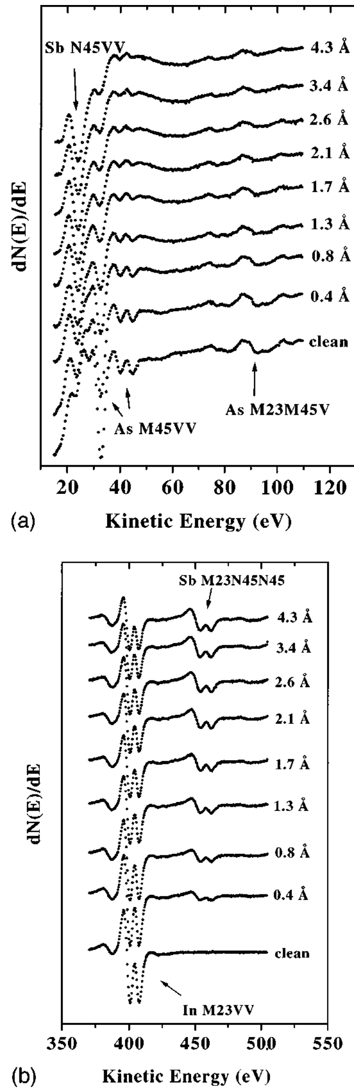

FIG. 1. (a) Auger As $M_{45}VV$, Sb $N_{45}VV$, As $M_{23}M_{45}V$ lines taken in the first derivative mode as a function of Sb coverage. (b) Auger In $M_{23}VV$ and Sb $M_{23}N_{45}N_{45}$ lines as a function of Sb coverage.

The InAs single crystals were n-type doped ($n=1\times10^{18}$ atoms/cm^3) bars and the (110) clean surfaces were obtained by cleaving *in situ*. Antimony shots were sublimated from a resistively heated quartz crucible at a low sublimation rate (0.5 ML/min). Thickness was measured by means of a quartz-crystal–thickness monitor and calibrated by means of Auger peak intensity. The ordered Sb monolayer was obtained after depositing 10 ML of Sb and heating the InAs crystal at 600 K for about 15 min. The temperature was monitored with a Chromel-Alumel thermocouple welded close to the surface. A (1×1) low-energy electron diffraction (LEED) pattern was present even at 4 ML although superimposed on a structureless background. After the described thermal treatment for obtaining the ordered monolayer, a distinct image was observed, without any background with respect to the LEED pattern of the 1 ML as deposited. One monolayer is defined as a Sb atomic density equivalent to the surface atomic density of InAs(110) (7.76×10^{14} atoms/cm^2) corresponding to 2.35 Å nominal thickness.

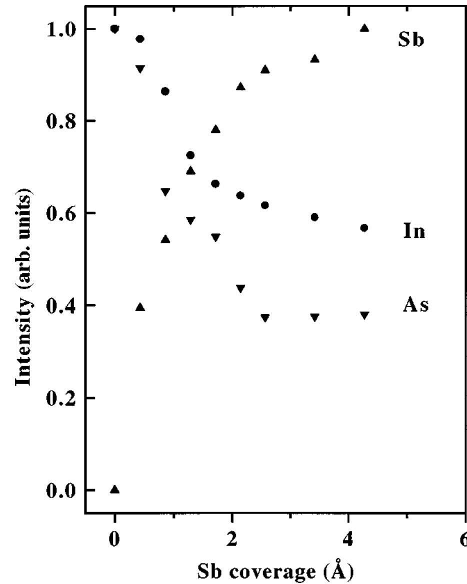

FIG. 2. Auger peak-to-peak intensities of As $M_{23}M_{45}V$, In$M_{23}VV$, and Sb $M_{23}N_{45}N_{45}$ Auger lines as a function of Sb coverage.

III. RESULTS AND DISCUSSION

A. Overlayer growth morphology and chemical bonding

The growth morphology of Sb deposited on the InAs(110) surface has been characterized by means of Auger electron spectroscopy. The evolution of the chemical bonding at the surface has been deduced by studying the line shape of photoemitted In $4d$ core levels.

The As $M_{45}VV$, Sb $N_{45}VV$, As $M_{23}M_{45}V$, In $M_{23}VV$, and Sb $M_{23}N_{45}N_{45}$ Auger lines taken in the first derivative mode are shown in Figs. 1(a) and 1(b) as a function of Sb coverage. The energy position and line shape of all the Auger peaks do not change in the whole coverage range indicating unreactivity of the growing interface, in agreement with what was been observed on several other Sb/III–V (110) interfaces.[5,11] The peak-to-peak intensities of a set of Auger lines are collected in Fig. 2 as a function of Sb coverage. We do not show the evolution of the As $M_{45}VV$ and Sb $N_{45}VV$ lines because they partially overlap. The lines evolution shows a slope change at about 2.3–2.4 Å, the lower coverage behavior being linear, the higher coverage range having a lower growth rate. This evolution denotes a Stranski-Krastanov (SK) growth mode, characterized by uniform formation of the first monolayer, followed by three-dimensional island growth, in agreement with Sb overlayer formation on several III–V (110) surfaces.[5,14] The corresponding LEED image shows a (1×1) pattern with low background at coverage larger than 1 ML, in agreement with previous work.[11] By fitting the experimental curves from Fig. 2 with a simple theoretical model for SK growth[15] characterized by the typical $\exp(-d/\lambda)$ behavior (with d the overlayer thickness and λ the electron mean-free path), we estimate electron mean-free path values of about 5.5 and 10.2 Å for the As and In Auger lines, respectively. The different λ value for the two lines is perfectly compatible with the different kinetic energy of the Auger peaks,[16] thus explaining that the

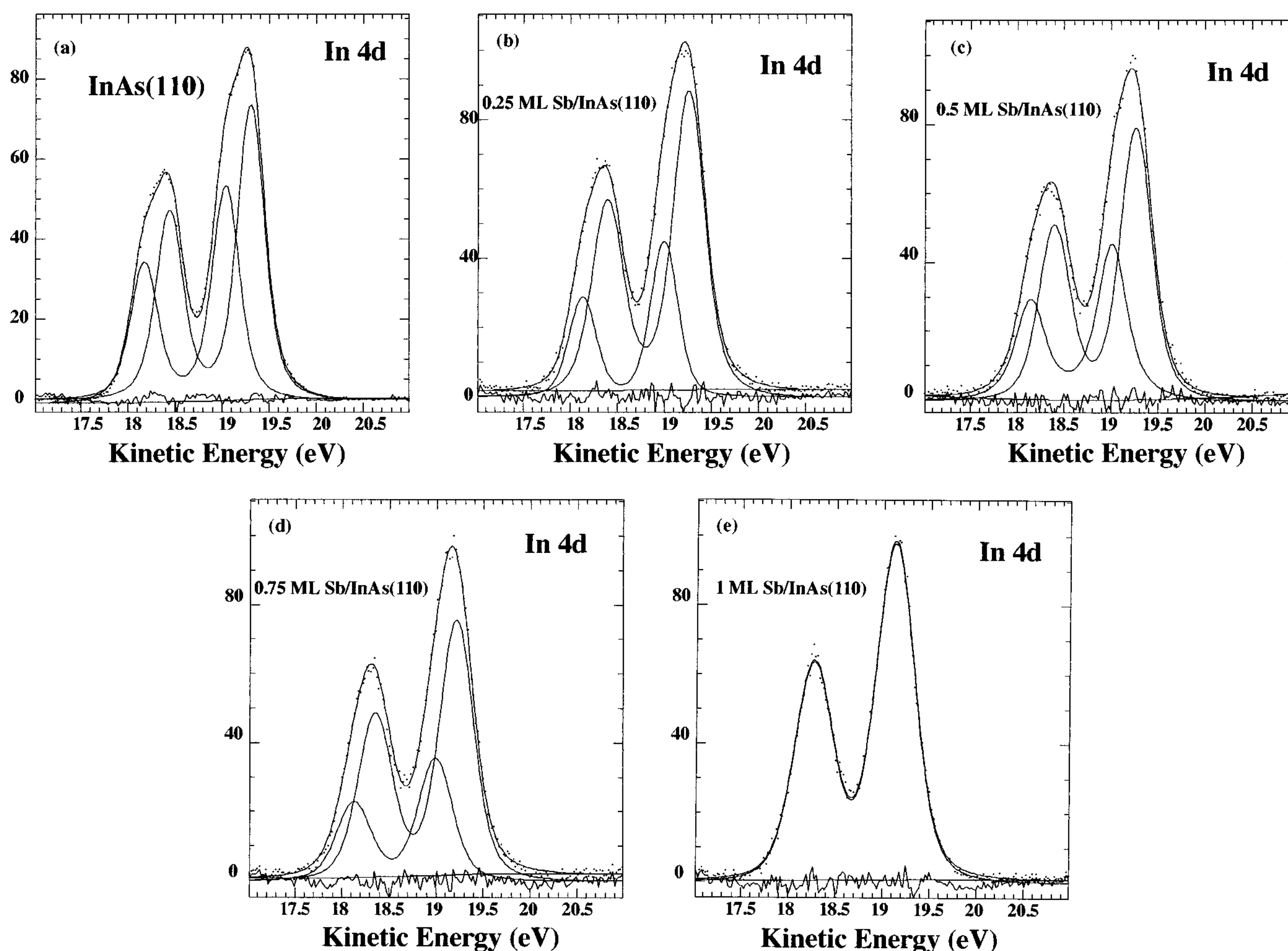

FIG. 3. (a)–(e) In $4d$ core-level normalized spectra as a function of Sb coverage (0–1 ML) at the Sb/n-type doped InAs(110) interface, taken at $h\nu = 40.8$ eV (He II). Experimental data (dots) are superimposed to the result of a deconvolution in surface and bulk components.

slow decrease of the As-to-In intensity ratio as a function of coverage does not indicate preferential bonding sites.

More information about chemical bonding can be accomplished through investigation of the line shape of the In $4d$ core levels as a function of Sb coverage, shown in Figs. 3(a)–3(e). Experimental data are superimposed to the final results of a deconvolution in different core-level components obtained by appropriate least-squares fitting procedure. It is clear that there are two spin-orbit split components in the clean InAs(110) spectrum, which can be attributed to bulk and surface emission. Each component has been fitted with a spin-orbit split doublet ($\Delta_{SO} = 0.86$ eV), with an intensity ratio of 1.57, intrinsic Lorentzian width of 0.18 eV, and Gaussian broadening of 0.24 eV. The surface core-level shift is 0.27 eV with respect to the bulk component (higher kinetic-energy component), in good agreement with previous investigation.[17] Main evidences upon antimony deposition are an energy shift of both surface and bulk core levels due to band bending (that will be commented on in Sec. III C) and an intensity reduction of the surface component. Data deconvolution including a third reacted component does not lead to realistic fit results. Thus, the best fittings shown in Figs. 3(a)–3(d) were obtained with two components and show a continuous reduction of the surface core levels, which disappear at the 1 ML coverage shown in Fig. 3(e). This confirms the unreactive nature of the Sb/InAs(100) interface and indicates counter relaxation of the underlying topmost InAs layer, in analogy with other Sb/III–V(110) interfaces.[18–20]

Well defined and ordered (1×1)-Sb monolayer is obtained via annealing of a 4-ML-thick adlayer, in analogy with other (1×1)-Sb ML's grown on III-V's(110).[5,14] Auger peak-to-peak intensities of the Sb, In, and As lines are plotted in Fig. 4 as a function of annealing temperature. A *plateau* in the temperature range 550–600 K indicates a stable chemisorption phase, corresponding to a very distinct (1×1) LEED image. The intensity ratio between Sb and substrate lines in this temperature range gives a thickness estimation of about 1 ML. This behavior again is in analogy with the prototypical well ordered (1×1)-Sb/GaAs(110) interface,[5] though in the latter case the ordered phase is stable up to more than 800 K.[5]

The In $4d$ core levels of the well-ordered (1×1)-Sb stable phase are shown in Fig. 5, compared to the same core levels for the 1-ML-as deposited. The best fitting leads to a single spin-orbit split component with a Gaussian broadening reduced from 0.37 to 0.28 eV, compared to the RT deposition of 1-ML Sb on InAs(110). This demonstrates the presence of a single chemical environment around the In atoms, consistent with a full derelaxation of the topmost InAs layer

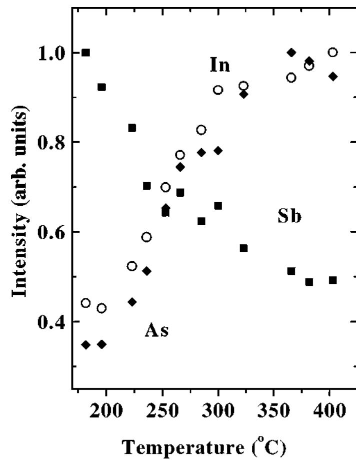

FIG. 4. Auger peak-to-peak intensity of the As $M_{23}M_{45}V$, In $M_{23}VV$, and Sb $M_{23}N_{45}N_{45}$ lines as a function of annealing temperature.

induced by the well-ordered Sb layer. Moreover, the lower Gaussian width with respect to the 1-ML-as deposited is consistent with a better order in the ML achieved by annealing.

The room-temperature growth morphology of Sb on InAs(110) is characterized by unreactivity, lack of interdiffusion, and absence of preferential bonding sites. After completion of a first laminar monolayer, antimony forms disordered islands. Appropriate annealing of an Sb multilayer produces a well-ordered (1×1)-epitaxial Sb monolayer, inducing derelaxation of the underlying InAs substrate.

B. Antimony-induced electronic states

The evolution of the energy distribution curves (EDC's) in the valence-band region as a function of Sb deposition is shown in Fig. 6(a). The angular-integrated EDC relative to the clean InAs(110) surface presents several features, positioned, respectively, at 0.9, 1.4, 2.2, 3.3, 4.9, and 6 eV below the valence-band maximum [15.5, 15.0, 14.2, 13.1, 11.5, and 10.4 kinetic energy (KE), respectively], which can be attributed to surface states. Previous theoretical calculations[3,4,21] and angular resolved photoemission studies[22,23] identified these surface features. We can assign the shoulder at 15.5-eV KE and the structure at 15.0 eV KE to the As dangling and backbond states, respectively (the surface states $A5$, $A4$ as reported in Ref. 4) and the feature at 14.2 eV KE to the anion surface state ($A3$) localized between the first and second layer. Moreover, the structures at 13.1–11.5 and 10.4 eV KE are both related to In atoms and can be referred to the states $C2$ and $C1$ localized in the first and in the second layer, respectively.

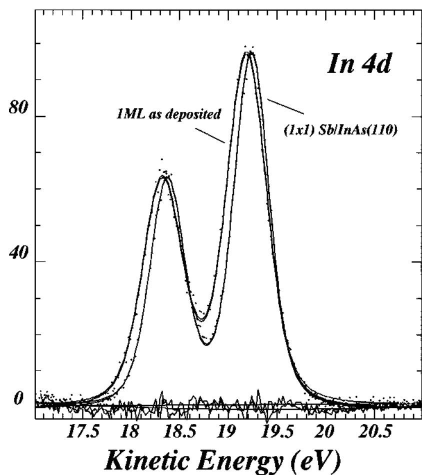

FIG. 5. The In $4d$ core levels of the ordered (1×1) Sb stable phase obtained by thermal annealing compared to the 1-ML Sb as deposited. Experimental data (dots) are superimposed to the result of a least-squares fitting analysis (see text).

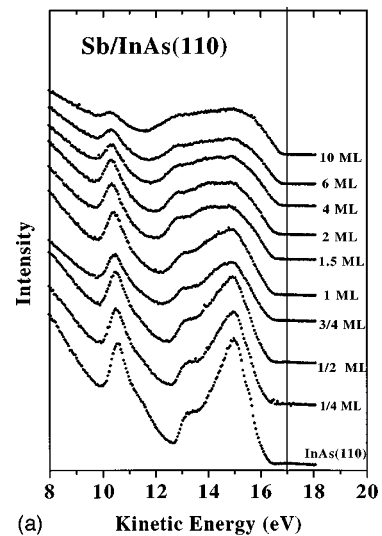

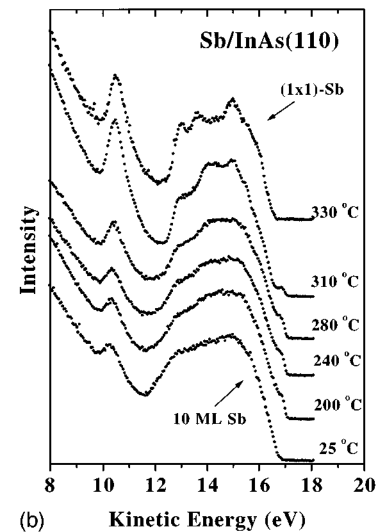

FIG. 6. (a) Angular integrated photoemission spectra in the valence-band region collected from InAs(110) at subsequent Sb deposition. (b) Angular integrated photoemission spectra collected from Sb/InAs(110) at subsequent annealing temperature. Photon energy of 21.2 eV (He I).

The antimony deposition induces a decreasing of all InAs(110) surface features in the valence-band region. A faint tail appears in the semiconductor bulk gap energy region, but there is no detectable density of states at the Fermi energy. The semiconducting character of the Sb/InAs(110) interface, still at high coverages (10 ML), is in agreement with previous results obtained on other Sb/III–V (110) systems.[24,25] In fact, antimony deposited on GaAs(110)

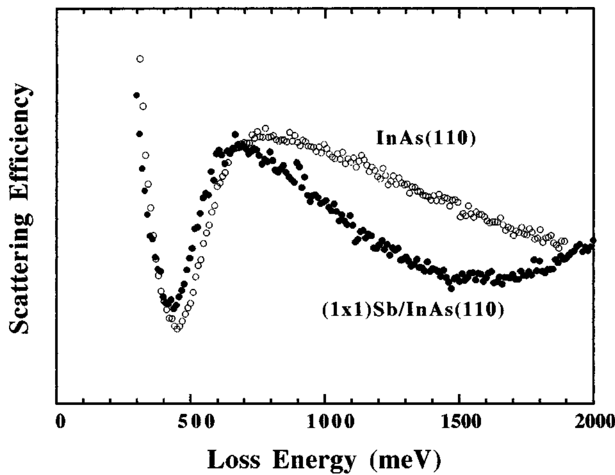

FIG. 7. Scattering efficiencies of HREELS in the energy-loss region of the semiconductor bulk gap for the clean InAs(110) surface and for the (1×1)-Sb ordered overlayer. Primary beam energy $E_p = 21.6$ eV. Spectra are normalized to the elastic peak height.

grows in the Stranski-Krastanov mode and the Sb islands coalesce in an amorphous layer. It is well known that a transition from a crystalline to an amorphous phase in Sb and As leads to a semimetal-semiconductor transition.[26]

The evolution of the photoemission EDC spectra at different annealing temperatures, starting from the 10-ML-thick Sb overlayer, is reported in Fig. 6(b). At the first annealing temperature Sb starts desorbing and a structure close to the Fermi level appears, probably due to an ordering of the Sb overlayer. Annealing at 525 K of a thick Sb layer on GaAs(110) leads to ordered overlayers with two distinct periodic superstructures (moire effect orientation[25]). An analogous reordering driven by the annealing can occur in the Sb amorphous overlayer deposited on InAs(110) giving rise to a semimetallic behavior with a low, but finite spectral density of states at the Fermi edge.

When antimony in excess of 1 ML fully desorbs leaving the ordered (1×1) layer at about 600 K, the Sb-induced states are well resolved and defined and the structure close to the Fermi level disappears. The main features that can be related to Sb-induced electronic states are at 16.0, 15.6, 14.95, 14.3, 13.6, 13.0, and 10.45 eV KE [corresponding to 0.9, 1.3, 1.95, 2.6, 3.3, 3.9, and 6.45 eV binding energy (BE) with respect to the Fermi level, respectively]. There is an overall fairly good agreement with previous experimental result[13] and band-structure calculation,[4,14] taking into account that our data are angle integrated, thus representing a partial integration of each band dispersion along the surface Brillouin zone. In particular, the two bumps at 16.0 and 15.6 KE (0.9 and 1.3 eV BE) can be related to the highest occupied Sb-induced level $S6$ (notation used in Ref. 4), the strong peak at 14.95 eV KE (1.95 eV BE) can be attributed to the $S5$ bonding surface state, the further structures at 14.3–13.6 and 13.0 eV KE (2.6–3.3 and 3.9 eV BE) can be identified with the Sb intrachain bonding $S4$ and $S3$ levels, respectively, and the peak at 10.45 eV KE (6.45 eV BE) is consistent with the $S2$ nonbonding Sb states.

The scattering efficiencies in the energy-loss region of the semiconductor bulk gap for the clean InAs(110) surface and for the (1×1)-Sb ordered overlayer are reported in Fig. 7.

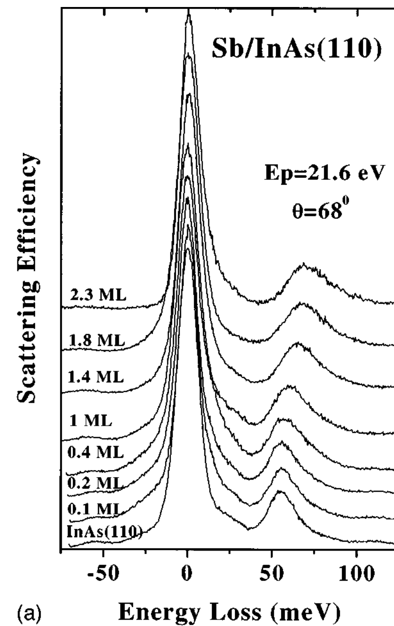

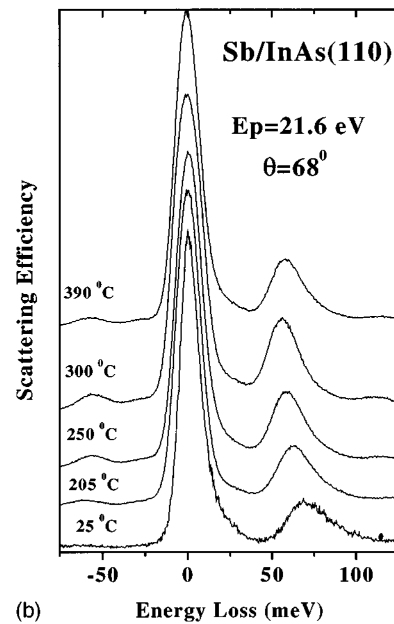

FIG. 8. Selection of HREELS spectra of the Sb/InAs(110) interface in the energy-loss region of collective excitations. Primary beam energy is 21.6 eV. Spectra are normalized to the elastic peak height and displaced along the vertical axes for convenience. (a) As a function of Sb coverage: notice how the phonon and plasmon loss energies shift to higher energy loss, (b) as a function of annealing temperature: the phonon and plasmon loss energies shift to lower energy loss.

High-resolution electron-energy-loss features in the semiconductor bulk gap energy region can be related to the electronic transitions involving occupied and empty surface or adatom-induced states. The clean InAs(110) surface exhibits a clear absorption structure with the onset at 450 meV. The main energy-loss feature peaks at about 750 meV and represents the maximum of the joint density of states, involving the filled and empty electronic surface states across the surface gap. Angular resolved photoemission on the clean InAs(110) (Refs. 22 and 23) surface singles out a filled surface state at

the $\bar{\Gamma}$ point, resonant with the bulk projected band, with downward dispersion to $\bar{X}$ and $\bar{X}'$. This surface state ($A5$) can be assigned to the initial state of the observed electronic transition at the edge, with an empty level (presumably $C3$) positioned at about 0.2 eV above the conduction-band minimum (CBM). Comparing the scattering efficiencies of the clean InAs(110) and the (1×1)-Sb ML on InAs(110), the surface electronic gap narrows to 420 meV, a broad absorption feature grows at about 675 meV, and a further structure is detectable at higher energy losses. The surface gap narrowing can be ascribed to the evolution of the Sb-induced states in the bulk gap, with the filled Sb-induced states ($S6$) slightly shifted towards the VBM in agreement with angular resolved photoemission results.[13] Moreover, the very low surface gap difference (30 meV) can be assumed as a sign of the very good 2D structural epitaxiality reflected in the sequence of occupied and empty electronic levels. Furthermore, from the energy-loss structure at 670 meV and the surface gap (420 meV) we can infer the minimum value for the position above CBM of the empty $S7$ state at about 250 meV. Band structure based on ECLS geometry derived from *ab initio* total-energy calculations[1] reveals a high density of filled states for $S5$ and $S6$ and for an empty state $S7$ at the critical point $\bar{X}'$, that can give rise to an interband transition at about 0.8 eV,[27] in fairly good agreement with our experimental determination.

Optical transitions of Sb/InAs(110) ordered structure have been measured in a higher energy range (1.2–6 eV) by means of reflectance anisotropy spectroscopy.[28] An absorption peak at 1.8 eV has been attributed to a transition from $S6$ to $S7$ Sb-induced states. In our opinion the discrepancy in this attribution might be due to the comparison with tight-binding (TB) band-structure calculations,[28] in fact the intrinsic inaccuracy of the TB method in determining energy dispersion of surface states is well known.

C. Space-charge layer formation and band bending

Antimony deposited on InAs(110), in analogy with the other unreactive and ordered Sb/III–V (110) interfaces, is also a model system to study the causes of the evolution of the space-charge layer in the underlying semiconductor surface. A pinning of the surface Fermi level for highly ordered interfaces can be only induced by the presence of the adlayer/metal–induced filled states in the semiconductor bulk gap. For epitaxial and unreactive systems such as Sb/III–V (110) we can monitor the evolution of the space-charge region during the formation of the interface and evaluate the effect of disorder and/or defect-induced states at different stages of the growth morphology.

The space-charge layer formation for the Sb/InAs(110) interface at subsequent Sb deposition and at different annealing temperature has been studied through core-level photoemission analysis and the collective excitations observed by HREELS. The shift of the In core-level bulk component gives information about the band-bending potential at the surface, while the variation of the charge density associated with the dopant-induced free-carrier plasmon can give insight into the accumulated or depleted charge at the surface.

A selected set of the scattering efficiencies of electron-energy-loss spectra, taken in the vibrational loss energy range at different Sb coverage, is collected in the left side of Fig. 8(a). In the clean nonpolar InAs(110) surface two plasmaron modes can be clearly resolved: the infrared-active transverse optical phonon at 26.9 meV and the plasmon loss due to the dopant-induced free-carrier plasmon at 55.2 meV. The deposition of antimony on the InAs(110) surface induces shift of the plasmaron excitations towards higher energy losses. The energy positions and the intensity modification of the ''plasmaron'' losses depend on the variation of the free-carrier density at the surface. If the electron density increases (decreases), as in an accumulation (depletion) layer, the plasmaron losses shift to higher (lower) loss energies. The blueshift observed depositing Sb indicates a carrier accumulation in the subsurface region. In the left panel of Fig. 9 the energy position of the plasmon loss, reported as a function of the Sb coverage, increases from 55.2 to 68 meV for the set of data taken at a primary beam energy of 21.6 eV.

The presence of an accumulation of carrier in the space-charge layer after the deposition of Sb on the InAs(110) surface can be confirmed through the analysis of core-level photoemission spectra. The In $4d$ core levels of the Sb/n-type doped InAs(110) doped interface as a function of Sb coverage (reported in the left panel of Fig. 3), show a shift of the centroid of the peaks to lower kinetic energy, achieved up to a coverage of 4 ML. At the clean n-type doped InAs(110) surface, the Fermi-level position has been measured at 0.17 eV above the conduction-band minimum (CBM), within our experimental uncertainty, in good agreement with the expected value at RT in the flat band condition [0.11 eV above CBM for InAs(110) with n-type doping $n=1\times10^{18}$ atoms/cm^3, and effective mass $m^*=0.022\,m_e$]. Since the interface is unreactive and nondisruptive and the core-level line-shape analysis shows only a reduction of the surface component, the In $4d$ core-level energy shifts can be related to the surface band bending. Thus we can correlate the In $4d$ energy position to the surface Fermi level as a function of Sb coverage, as reported in the left panel of Fig. 10. From the core-level analysis of the In bulk component, we deduced an energy shift of about 200 meV towards higher kinetic energy. After the deposition of 2 ML of Sb, the Fermi level enters by about 350 meV into the conduction band, leading to a band-bending potential due to the accumulated charge layer. This result is in fairly good agreement with previous band-bending measurements.[12,29,30] The maximum value of the downward band bending for the accumulation layer occurs at the same Sb coverage for which the highest energy-loss shift of the plasmon mode is achieved, as can be observed by comparing the left panels of Figs. 9 and 10. The formation of an accumulation layer with a Fermi level pinned into the conduction band has been already observed on other metal/narrow gap semiconductor interfaces, like Cs and Ag deposited on InAs(110),[29,31] or Ag and Cs on InSb(110).[32,33] Recent photoemission data reveal the presence of native defect states in the conduction band of clean uncleaved InAs surfaces inducing an accumulation layer.[34] For the clean InAs surfaces it was proposed that cation antisites defects induce the pinning of the Fermi level above the CBM and their charge is transferred into the lower laying states at the CBM.[35] For the Sb/n-type doped GaAs(110) interface, the pinning of the Fermi level induces a depletion

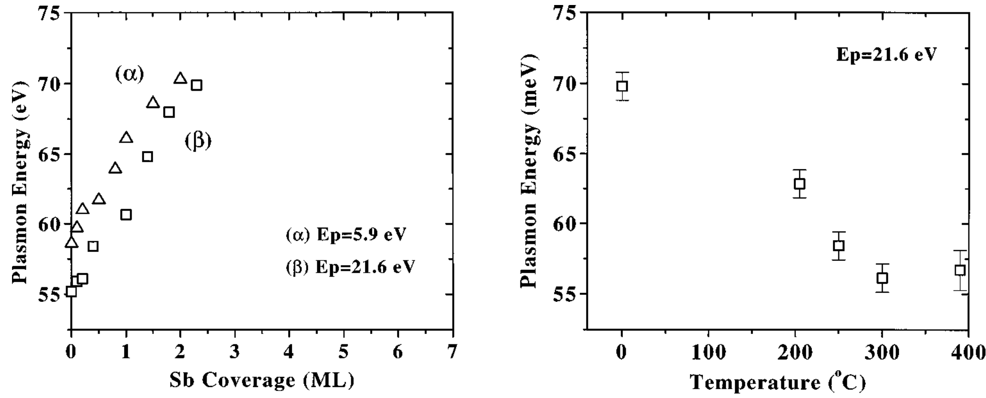

FIG. 9. Plasmon energy position for the Sb/InAs(110) interface at room temperature and at different primary beam energies as a function of Sb coverage (left panel), and as a function of annealing temperature (right panel).

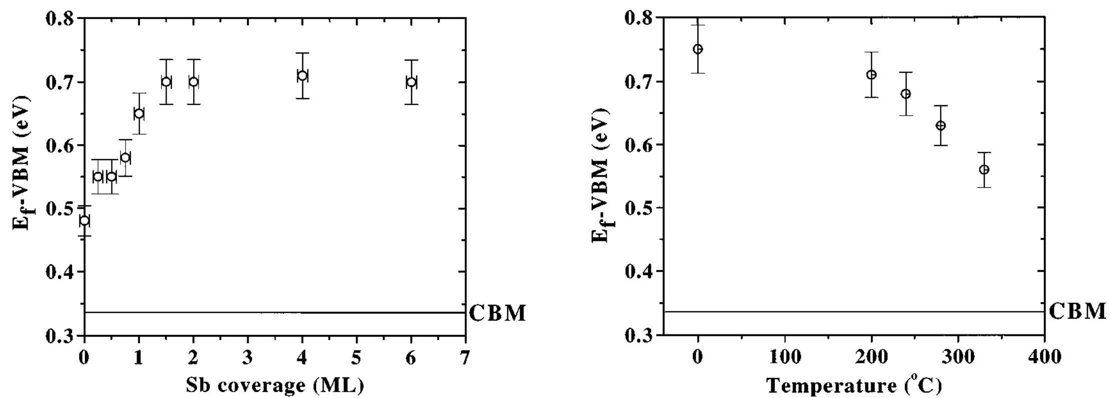

FIG. 10. Surface Fermi-level position with respect to the conduction-band minimum at the n-type doped InAs(110) surface at room temperature as a function of Sb coverage (left panel), and as a function of annealing temperature (right panel). The zero energy corresponds to the VBM, the horizontal line marks to the CBM position.

layer attributed to states due to unsaturated dangling bonds localized at the edge of the Sb terraces. As observed by scanning tunneling spectroscopy.[6,35] Antimony can induce on the n-type InAs(110) surface defect-donor states, in analogy with Sb/GaAs(110) interface. These defect states can be positioned above the conduction-band minimum, inducing the formation of an accumulation of carriers at the surface, as has been observed for uncleaved InAs surfaces.[34,35]

Annealing of 4-ML Sb/n-type doped InAs(110) leads to a large reduction of the band bending from 350 to 180 meV above CBM towards the flat band condition as shown in the right panel of Fig. 10. The same behavior can be observed from the plasmaron excitations in the HREELS spectra as shown in the right panel of Fig. 9. The plasmon energy suddenly shifts to lower loss energy at 470 K, indicating a decrease of the charge accumulated at the surface.

The effect of the reduced band bending upon annealing can be explained by the formation of a stable highly ordered (1×1) Sb monolayer where the defect states are quenched. The highly ordered (1×1) Sb deposited on GaAs(110) shows an analogous decreasing of the band bending due to a reduction of the defects states with respect to the monolayer as deposited.[36,37] The absence of the Sb induced filled states in the bulk gap and the disappearance of the donor-defect states for the highly ordered (1×1) Sb/InAs(110) induce a nearly flat band condition without charging at the surface.

IV. CONCLUSIONS

Semimetal antimony deposited on III–V (110) surfaces is an example of highly ordered interfaces where the electronic and structural properties are easily comparable with theoretical results. These are also model systems for understanding the Schottky barrier formation, elucidating the role of defect states in the adlayer growth. Antimony deposited on InAs(110) belongs to this family, showing an epitaxial growth at RT, characterized by unreactivity, lack of interdiffusion, and absence of preferential bonding sites. Appropriate annealing of a multilayer Sb produces a well-ordered (1×1)-Sb monolayer with a surface gap at 420 meV. During the growth of the Sb layer, the presence of donor defect states induces an accumulation layer that is considerably reduced when the annealing process gives rise to a highly ordered (1×1) interface, quenching the defects at the surface.

ACKNOWLEDGMENT

This work was supported by the ''Progetto di ricerca avanzata'' (Advanced Research Project) of the Università degli Studi di Modena.

[1] W. Gero Schmidt, F. Bechstedt, and G. P. Srivastava, Surf. Sci. Rep. **25**, 141 (1996), and references therein; J. P. LaFemina, *ibid.* **16**, 133 (1992), and references therein.
[2] Maria Grazia Betti, Phys. Low Dimens. Struct. **12**, 71 (1995), and references therein.
[3] J. E. Northrup, Phys. Rev. B **44**, 1349 (1991).
[4] C. Mailhiot, C. B. Duke, and D. J. Chadi, Phys. Rev. B **31**, 2213 (1985).
[5] J. Carelli and A. Kahn, Surf. Sci. **116**, 280 (1982).
[6] R. M. Feenstra and P. Mårtensson, Phys. Rev. Lett. **61**, 447 (1988).
[7] C. B. Duke, A. Paton, W. K. Ford, A. Kahn, and J. Carelli, Phys. Rev. B **26**, 803 (1982).
[8] P. Mårtensson, G. V. Hansson, M. M. Låhdeniemi, K. O. Magnusson, S. Wiklund, and J. M. Nicholls, Phys. Rev. B **33**, 7399 (1986).
[9] M. G. Betti, C. Mariani, N. Jedrecy, R. Pinchaux, A. Ruocco, and M. Sauvage-Simkin, Phys. Rev. B **50**, 14 336 (1994).
[10] M. G. Betti, M. Pedio, U. del Pennino, and C. Mariani, Phys. Rev. B **45**, 14 057 (1992).
[11] W. K. Ford, T. Guo, S. L. Lantz, K. Wan, S.-L. Chang, C. B. Duke, and D. L. Lessor, J. Vac. Sci. Technol. B **8**, 940 (1990).
[12] C. Novak, J. Krujatz, A. Markl, C. Meyne, A. Chassé, W. Braun, W. Richter, and D. R. T. Zahn, Surf. Sci. **331–333**, 619 (1995).
[13] A. B. McLean, D. M. Swanston, D. N. McIlroy, D. Heskett, R. Ludeke, and H. Munekata, Phys. Rev. B **51**, 14 271 (1995).
[14] W. Gero Schmidt and G. P. Srivastava, Surf. Sci. **331–333**, 540 (1995).
[15] S. Ossicini, T. Memeo, and F. Ciccacci, J. Vac. Sci. Technol. A **3**, 387 (1985).
[16] M. P. Seah and W. A. Dench, Surf. Interface Anal. **1**, 2 (1979).
[17] A. B. Mc Lean, J. Phys.: Condens. Matter **2**, 1027 (1990).
[18] F. Schaeffler, R. Ludeke, A. Taleb-Ibrahimi, G. Hughes, and D. Rieger, J. Vac. Sci. Technol. B **5**, 1048 (1987).
[19] T. Kendelewicz, K. Miyano, R. Cao, I. Lindau, and W. E. Spicer, J. Vac. Sci. Technol. B **11**, 991 (1989).
[20] N. Esser, D. R. T. Zahn, C. Mueller, W. Richter, R. Whittle, I. T. McGovern, S. Kularni, and W. Braun, Appl. Surf. Sci. **56–58**, 169 (1992).
[21] J. L. A. Alves, J. Hebenstreit, and M. Scheffler, Phys. Rev. B **44**, 6188 (1991).
[22] C. B. Andersson, J. N. Andersen, P. E. S. Persson, and U. O. Karlsson, Phys. Rev. B **47**, 2427 (1993).
[23] D. M. Swanston, A. B. Mc Lean, D. N. Mc Ilroy, D. Heskett, R. Ludeke, H. Munekata, M. Prietsch, and N. J. DiNardo, Surf. Sci. **312**, 361 (1994).
[24] G. Annovi, Maria Grazia Betti, U. del Pennino, and Carlo Mariani, Phys. Rev. B **41**, 11 798 (1990).
[25] J. C. Patrin, Y. Z. Li, M. Chandler, and J. H. Weaver, Phys. Rev. B **46**, 10 221 (1992); **46**, 3918 (1992).
[26] X. Pollak, S. P. Kowalczyk, R. McFeely, and D. A. Shirley, Phys. Rev. B **8**, 641 (1973).
[27] *Ab initio total* energy calculations for InAs(110) give an underestimation of the lattice constants and a subsequent overestimation of the excitation energies as explained in Ref. 1, pp. 188–189. The fundamental band gap for bulk InAs at zero temperature results in 0.86 eV instead of 0.42 eV as deduced by experimental results. By applying the same energy shift to the estimated electronic transition at the critical point $\bar{X}'$ (1.25 eV), we obtain the transition energy at about 0.8 eV.
[28] A. I. Shkrebtii, N. Esser, M. Kopp, P. Haier, W. Richter, and R. Del Sole, Appl. Surf. Sci. **104/105**, 176 (1996).
[29] V. Yu Aristov, M. Grehk, V. M. Zhilin, A. Taleb-Ibrahimi, G. Indlekofer, Z. Hurych, G. LeLay, and P. Soukiassian, Appl. Surf. Sci. **10/105**, 73 (1996).
[30] V. Yu Aristov, G. LeLay, P. Soukiassian, K. Hricovini, J. E. Bonnet, J. Osvald, and O. Olsson, Europhys. Lett. **26**, 359 (1994).
[31] V. Yu Aristov, G. LeLay, Le Than Vihn, K. Hricovini, and J. E. Bonnet, Phys. Rev. B **47**, 2138 (1993).
[32] V. Yu Aristov, M. Bertolo, P. Althainz, and K. Jacobi, Surf. Sci. **281**, 74 (1993).
[33] Maria Grazia Betti, R. Biagi, U. del Pennino, M. Pedio, and Carlo Mariani, Phys. Rev. B **53**, 13 605 (1996).
[34] L. Ö. Olsson, C. B. M. Andersson, M. C. Håkansson, J. Kanski, L. Ilver, and U. O. Karlsson, Phys. Rev. Lett. **76**, 3626 (1996).
[35] W. Pötz and D. K. Ferry, Phys. Rev. B **31**, 968 (1985).
[36] R. M. Feenstra, Appl. Surf. Sci. **56–58**, 104 (1992).
[37] N. Esser, M. Reckzügel, R. Srama, U. Resch, D. R. T. Zahn, W. Richter, C. Stephens, and M. Hünermann, Appl. Surf. Sci. **56–58**, 169 (1992).